

Efficient Capping of Growing Gold Nanoparticles by Porphyrin Having Two Disulfide Straps over One Face

Yutaka Hitomi,*[1] Junya Ohyama,[2] Yasuhiro Higuchi,[2] Kazuki Aoki,[1] Tetsuya Shishido,[2] Takuzo Funabiki,[1] Masahito Kodera,[1] and Tsunehiro Tanaka[2]

[1]Department of Molecular Chemistry and Biochemistry, Doshisha University, Kyotanabe, Kyoto 610-0321

[2]Department of Molecular Engineering, Graduate School of Engineering, Kyoto University, Kyoto Daigaku Katsura, Nishikyo-ku, Kyoto 606-8501

Received June 10, 2010; E-mail: yhitomi@mail.doshisha.ac.jp

Two types of tetrathiolated surface passivants were synthesized in order to explore the effect of *S*-functional groups (disulfide vs. *S*-thioester) to control the size of gold nanoparticles prepared by a simple one-pot reduction of tetrachloroaurate with sodium tetrahydroborate. Both the passivants have four thiolated arms in the same direction perpendicular to a porphyrin plane, and produced small porphyrin-coated gold nanoparticles 2 to 4 nm in size by one-pot reduction of Au^{III} ions at S/Au from 1 to 16. The constancy in particle size at S/Au ratio less than 4 was greater with use of tetradentate disulfide passivant compared with use of tetradentate *S*-thioester ligand, which should be attributed to faster adsorption of disulfide groups with gold than that of *S*-thioester groups. The results described here suggest that passivants having multivalent disulfide bonds should be promising candidates for constructing monolayer-protected gold nanoparticles of well-defined size.

Nanosized gold particles have attracted increasing attention because they display unique properties that are not observed in bulk gold, such as distinctive extinction bands in the visible region and catalytic activities.[1–3] The properties are highly dependent on particle size; therefore, substantial efforts have been made to develop methods of preparing gold nanoparticles with a desired size. In general, small gold nanoparticles or nanoclusters have been prepared by reduction of gold ions in presence of polymers or high-surface-area metal oxides; these adsorbents suppress growth and agglomeration of gold nanoparticles owing to their weak but numerous interaction points with gold. The use of a large excess of surface passivants such as 1-dodecanethiol is another strategy to synthesize gold nanoparticles with a controlled small particle size.[3–9] In this case, the initial molar ratio of alkanethiols and gold ions is crucial to determining the particle size; increasing the molar ratio decreases the particle size.[8,10] The resulting monolayer-protected gold nanoparticles are attractive in designing nanoscale devices such as memory devices, sensors, and catalysts because of their ability to introduce various types of functional molecules.[1–3,11–17]

The use of surface passivants that can afford multiple Au–S interactions has been employed by several groups in effort to stabilize gold nanoparticles. Jutzi and co-workers improved the exchange stability of thiolate ligands on gold nanoparticles using a tridentate alkanethiol, 1,1,1-tris(mercaptomethyl)-undecane.[18] Lee and co-workers reported that bidentate and particular tridentate alkanethiols inhibit the aggregation of large gold nanoparticles in organic solvents.[19–21] Wei and co-workers succeeded in stabilization of large gold nanoparticles up to 87 nm using resorcinarene tetrathiols.[22] Mayor, Simon, and co-workers have synthesized a series of linear oligomeric multidentate thioether ligands, and demonstrated the advantage of multidentate ligands in enwrapping and stabilizing gold nanoparticles with diameters below 2 nm, which become more stable with increasing the number of the thioether groups.[23] Kanehara and co-workers reported that porphyrin derivatives having four thioester groups, tetrakis-5,10,15,20-(2-acetylthiophenyl)-porphyrin, **SC_0P**, and tetrakis-5,10,15,20-(2-acetylthiomethylphenyl)porphyrin, **SC_1P**, can stabilize gold nanoparticles even under the ligand-exchange conditions.[17] Thus, multidentate ligands have been shown to be able to stabilize gold nanoparticles in an effective manner. Recently, we reported the synthesis of a tetradentate surface passivant **1^{SAc}** holding up four *S*-thioester arms in the same direction perpendicular to a porphyrin plane in order to introduce porphyrin molecules in a well-defined orientation on a gold surface (Scheme 1).[24] The porphyrin **1^{SAc}** has a structure related to Kanehara's porphyrins, **SC_nP**. The porphyrins **SC_nP** are a mixture of four atropisomers, but **1^{SAc}** has only a stable $\alpha,\alpha,\alpha,\alpha$-atropisomer. This advantage enables us to synthesize porphyrin-coated gold nanoparticles through one-pot reduction at room temperature.[17,24] Reduction of a DMF solution containing a 1:4 molar ratio of Au^{III} ions and

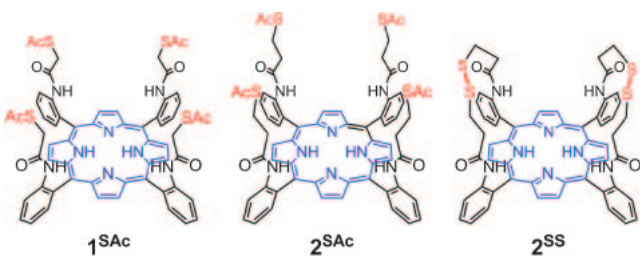

Scheme 1. Structures of porphyrin-based passivants.

Published on the web October 21, 2010; doi:10.1246/bcsj.20100160

$\mathbf{1}^{\mathbf{SAc}}$ affords ca. 2-nm gold nanoparticles, which is significantly smaller than those prepared using 1-dodecanethiol instead of $\mathbf{1}^{\mathbf{SAc}}$ at the same molar ratio of S atoms and Au^{III} ions.[24] This result suggests that multidentate passivants not only stabilize gold nanoparticles but also would provide a unique opportunity to alter the nucleation and growth processes of gold nanoparticles. Herein, we synthesized a new porphyrin-based passivant $\mathbf{2}^{\mathbf{SS}}$ which can give small gold nanoparticles at much smaller molar ratio of S atoms and Au ions than the previously reported passivant $\mathbf{1}^{\mathbf{SAc}}$.

Experimental

Materials. 2-Nitrobenzaldehyde, pyrrole, *N*,*N*-diethylaniline, and thioacetic acid were purchased from Tokyo Chemical Industry (Tokyo, Japan), and the other chemicals and solvents were from Wako Pure Chemical Industry (Osaka, Japan).

Instrumentation. Electronic absorption spectra were measured on a HITACHI U-3500 UV-VIS-NIR spectrometer by using a quartz cell with a 1-cm path length. ^{1}H, ^{13}C, 2D (HMQC, HMBC) NMR spectra were measured in $CDCl_3$ (expect for $\mathbf{2}^{\mathbf{SS}}$) and DMSO-d_6 ($\mathbf{2}^{\mathbf{SS}}$) on a JEOL JNM-ECX400 spectrometer. Transmission electron microscopy (TEM) images were taken with a JEOL JEM-100SX operating at an accelerating voltage of 100 kV and a JEOL JEM-2100F operating at an accelerating voltage of 200 kV. TEM samples were prepared by depositing drops of a methanol solution onto a carbon-coated copper grid (Okenshoji Co.) and dried at room temperature. At least 200 particles were measured to determine the mean diameter. X-ray photoelectron spectroscopy (XPS) measurement was performed using an ULVAC PHI 5500MT. XPS samples were mounted on an indium foil and the spectra were measured using Mg Kα radiation (15 kV, 400 W) in a chamber with the base pressure of ca. 1×10^{-8} Torr. The take-off angle was set at 45°. All binding energies were corrected for charge shifting by referencing to the C(ls) line from the adventitious carbon at 284.6 eV.

Synthesis of $\mathbf{2}^{\mathbf{SAc}}$. To a solution of $\alpha,\alpha,\alpha,\alpha$-5,10,15,20-tetrakis(*o*-acrylamidophenyl)porphyrin[25] (0.212 g, 0.238 mmol) in dry CH_2Cl_2 (2 mL) were thioacetic acid (210 µL, 2.95 mmol) and dry triethylamine (60 µL, 0.430 mmol) added. After the solution was stirred for 2 h at room temperature, the solvent was removed under reduced pressure. The residue was purified by column chromatography on silica gel eluted with 3 vol % MeOH in $CHCl_3$ and subsequent recrystallization from $CHCl_3$/MeOH to afford $\mathbf{2}^{\mathbf{SAc}}$ (64%). TLC: $R_f = 0.32$ ($CHCl_3$:MeOH = 30:1); HRMS-FAB (m/z): $[M + H]^+$ calcd for $C_{64}H_{59}O_8N_8S_4$, 1194.3260; found, 1194.3302; ^{1}H NMR ($CDCl_3$, 400 MHz): δ 8.81 (s, 8H), 8.65 (d, $J = 7.5$ Hz, 4H), 7.93 (d, $J = 8.0$ Hz, 4H), 7.87–7.82 (m, 4H), 7.54–7.52 (m, 4H), 7.12 (s, 4H), 2.55 (brs, 8H), 1.71 (brs, 8H), 1.60 (s, 12H), −2.73 (s, 2H); ^{13}C NMR ($CDCl_3$, 100 MHz): δ 195.6 (C_j), 165.9 (C_g), 138.2 (C_e), 135.1 (C_d), 131.8 (C_f), 131.4 (C_m), 130.1 (C_c), 123.6 (C_b), 122.1 (C_a), 115.2 (C_l), 36.0 (C_h), 30.0 (C_k), 24.5 (C_i) (The *meso*-carbon atoms, C_n, could not be observed, presumably due to N–H tautomerism.[26]); UV–vis λ_{max} in DMF: 423, 517, 550, 591, 648 nm.

Synthesis of $\mathbf{2}^{\mathbf{SS}}$. To a solution of $\mathbf{2}^{\mathbf{SAc}}$ (0.100 g, 0.0837 mmol) in THF (100 mL) was 25% NH_3 aq. (13 mL) added. After the mixture was stirred for 1 day at room temperature, the solvent was removed under reduced pressure. The residue was dissolved in $CHCl_3$ and washed with water. The aqueous phase was washed with $CHCl_3$ and all the organic phase was collected. The organic phase was dried over Na_2SO_4, and filtered to be concentrated under reduced pressure. The residue was purified by column chromatography on silica gel eluted with 9 vol % CH_3OH in $CHCl_3$ and subsequent recrystallization from $CHCl_3$/MeOH to afford $\mathbf{2}^{\mathbf{SS}}$ (65%). TLC: $R_f = 0.48$ ($CHCl_3$:MeOH = 10:1); HRMS-FAB (m/z): $[M]^+$ calcd for $C_{56}H_{46}O_4N_8S_4$, 1022.2525; found, 1022.2523; ^{1}H NMR (DMSO-d_6, 400 MHz): δ 8.73 (s, 8H), 8.64 (s, 4H), 8.34 (d, $J = 8.0$ Hz, 4H), 7.87–7.81 (m, 8H), 7.56–7.52 (m, 4H), 2.27–2.09 (m, 8H), 2.06–1.79 (m, 8H), –2.73 (s, 2H); ^{13}C NMR (DMSO-d_6, 100 MHz): δ 168.8 (C_g), 138.0 (C_e), 135.8 (C_d), 133.3 (C_f), 131.0 (C_k), 129.1 (C_c), 123.5 (C_b), 123.2 (C_a), 115.4 (C_j), 34.6 (C_i), 32.3 (C_h) (The *meso*-carbon atoms, C_l, could not be observed, presumably due to N–H tautomerism.[26]); UV–vis λ_{max} in DMF: 423, 516, 551, 593, 649 nm.

X-ray Structure Determination of Zinc Complex of $\mathbf{2}^{\mathbf{SS}}$. Crystals for X-ray analysis were grown by the slow diffusion of methanol into a chloroform solution of zinc complex of $\mathbf{2}^{\mathbf{SS}}$, **Zn-$\mathbf{2}^{\mathbf{SS}}$**, which was prepared by reacting $\mathbf{2}^{\mathbf{SS}}$ with $Zn(OAc)_2$ in $CHCl_3$ at room temperature. $C_{57}H_{47}Cl_3N_8O_5S_4Zn$, $M_r = 1224.03$, monoclinic, space group $P2_1/c$ (No. 14), $a = 13.2277(7)$, $b = 26.6609(14)$, $c = 16.2075(8)$ Å, $\alpha = \gamma = 90°$, $\beta = 107.5754(14)°$, $V = 5449.0(5)$ Å^3, $Z = 4$, μ(Mo Kα) = 0.378 mm^{-1}. Data collection ($6.06 < 2\theta < 55.24°$) was performed at 243 K using a Rigaku CCD diffractometer (Mo Kα, $\lambda = 0.71070$ Å). The structure was solved using direct methods and refined by a full-matrix least-squares method, giving a final R_1 value of 0.0755 for 768 parameters and 12444 unique reflections with $I > 2\sigma(I)$ and wR_2 of 0.1526 for all 12444 reflections. All non-hydrogen atoms and hydrogen atoms were anisotropically and isotropically refined, respectively. Crystallographic data have been deposited with Cambridge Crystallographic Data Centre: Deposition number CCDC-775279 for **Zn-$\mathbf{2}^{\mathbf{SS}}$**. Copies of the data can be obtained free of charge via http://www.ccdc.cam.ac.uk/conts/retrieving.html (or from the Cambridge Crystallographic Data Centre, 12, Union Road, Cambridge, CB2 1EZ, U.K.; Fax: +44 1223 336033; e-mail: deposit@ccdc.cam.ac.uk).

Gold Nanoparticles Covered with $\mathbf{2}^{\mathbf{SAc}}$, GN@$\mathbf{2}^{\mathbf{SAc}}$. To a solution of $\mathbf{2}^{\mathbf{SAc}}$ (18.0 mg, 15.0 µmol at $\xi = 1$ or 1.8 mg, 1.50 µmol at $\xi = 0.1$, in which ξ denotes the S/Au ratio) in DMF (292 mL) in a 500 mL round-bottom flask which was cleaned with piranha solution was added a 20.5 µM $HAuCl_4$ solution in DMF (0.5 mL). Then, the mixture was reduced with $NaBH_4$ (27.34 mg, 723 µmol) dissolved in DMF (7 mL). After stirring for 1.5 h, the reaction mixture was evaporated to ca. 3 mL and precipitated with 30 mL of methanol to remove excess $\mathbf{2}^{\mathbf{SAc}}$ and any salts. The precipitate was dissolved in DMF (3 mL) and precipitated again by adding $CHCl_3$ (30 mL). The reprecipitation process was repeated four times. The pure **GN@$\mathbf{2}^{\mathbf{SAc}}$** was characterized by TEM, UV–vis, and XPS measurements.

Gold Nanoparticles Covered with $\mathbf{2}^{\mathbf{SS}}$, GN@$\mathbf{2}^{\mathbf{SS}}$. **GN@$\mathbf{2}^{\mathbf{SS}}$** was prepared under the identical conditions to **GN@$\mathbf{2}^{\mathbf{SAc}}$**.

Size-Controlled Synthesis of Gold Nanoparticles. Gold nanoparticles were synthesized in the presence of $\mathbf{2}^{\mathbf{SAc}}$ and $\mathbf{2}^{\mathbf{SS}}$

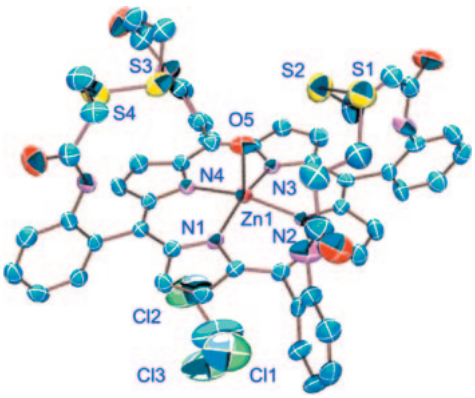

Figure 1. An ORTEP drawing of the zinc complex of $\mathbf{2}^{\mathbf{SS}}$ ($[Zn(\mathbf{2}^{\mathbf{SS}})(H_2O)]\cdot CHCl_3$) showing 50% probability thermal ellipsoids. The hydrogen atoms are omitted for clarity. Selected bond lengths/Å: S(1)–S(2) = 2.021(2), S(3)–S(4) = 2.020(4), Zn(1)–N(1) = 2.058(3), Zn(1)–N(2) = 2.081(4), Zn(1)–N(3) = 2.062(3), Zn(1)–N(4) = 2.069(4), Zn(1)–O(5) = 2.114(5).

under various molar ratios (S/Au = 0, 0.1, 0.2, 1, 4, and 16). All of glass vials for the syntheses of gold nanoparticles were cleaned with piranha solution. A typical method is as follows; an 1.0 mM solution of $\mathbf{2}^{\mathbf{SAc}}$ in DMF (8 mL, 8.00 μmol), a 153.7 mM solution of $HAuCl_4$ in DMF (13.0 μL, 2.00 μmol) and 1.8 mL of DMF were added to a reaction vessel. While the mixture was vigorously stirring, 100 μL of 241 mM $NaBH_4$ (24.1 mmol) was swiftly added and then stirred for 1 h. The solutions were evaporated and the residue was dispersed in MeOH.

Results and Discussion

Design and Synthesis of New Passivants. The previously reported porphyrin-based surface passivant $\mathbf{1}^{\mathbf{SAc}}$ has four *S*-thioester groups, but the XPS analysis indicated that the S atoms lack acetyl groups and exist as thiolate anions on a gold surface.[24] *S*-Thioester groups do not adsorb onto a gold surface rapidly compared to the corresponding thiol functional groups.[27,28] Therefore, we tried to deprotect the acetyl groups of $\mathbf{1}^{\mathbf{SAc}}$ in an attempt to realize more efficient capping of small gold nanoparticles. Unfortunately however, we failed to isolate any monomeric porphyrin compounds, instead always obtaining insoluble polymers, probably due to the formation of intermolecular disulfide bonds.[29] We then designed a new porphyrin-based passivant $\mathbf{2}^{\mathbf{SAc}}$ that has a structure similar to $\mathbf{1}^{\mathbf{SAc}}$ except for one more methylene in each arm (Scheme 1). Ligand $\mathbf{2}^{\mathbf{SAc}}$ was synthesized by Michael reaction of α,α,α,α-5,10,15,20-tetrakis(2-acryloylaminophenyl)porphyrin[24] and potassium thioacetate. Mild hydrolysis of $\mathbf{2}^{\mathbf{SAc}}$ followed by aeration nearly quantitatively yielded monomeric porphyrin compound $\mathbf{2}^{\mathbf{SS}}$, which has two disulfide bonds over one face of the porphyrin plane (Scheme 1). The C_2 symmetric structure of $\mathbf{2}^{\mathbf{SS}}$ was confirmed by ^1H and ^{13}C NMR measurements and by X-ray crystal structure analysis of the corresponding zinc complex (Figure 1).

Preparation and Absorption Spectra of Gold Nanoparticles. Porphyrin-coated gold nanoparticles were synthesized by $NaBH_4$ reduction of $HAuCl_4$ in a DMF solution containing $\mathbf{2}^{\mathbf{SAc}}$ or $\mathbf{2}^{\mathbf{SS}}$ at an S/Au ratio (ξ) of 1, hereafter called $\mathbf{GN@2}^{\mathbf{SAc}}$ or $\mathbf{GN@2}^{\mathbf{SS}}$, respectively. Both $\mathbf{GN@2}^{\mathbf{SAc}}$ and $\mathbf{GN@2}^{\mathbf{SS}}$ were purified by repeated precipitation with methanol and chloroform, as previously reported for $\mathbf{GN@1}^{\mathbf{SAc}}$.[23] The UV–vis spectra of $\mathbf{2}^{\mathbf{SAc}}$ and $\mathbf{2}^{\mathbf{SS}}$ were nearly identical (Figure 2A), but the gold nanoparticles prepared with them showed different features in the absorption spectra especially in surface plasmon bands. The UV–vis spectrum of purified $\mathbf{GN@2}^{\mathbf{SAc}}$ in a DMF solution showed a Soret band at 426.0 nm and a relatively weak, broad surface plasmon band at around 545 nm, which is very close to that of $\mathbf{GN@1}^{\mathbf{SAc}}$.[23] On the other hand, purified $\mathbf{GN@2}^{\mathbf{SS}}$ displayed an intense Soret band at 426.4 nm, but the surface plasmon band was fairly weak in intensity compared to those of $\mathbf{GN@1}^{\mathbf{SAc}}$ and $\mathbf{GN@2}^{\mathbf{SAc}}$ (Figure 2B). These results suggest that disulfide passivant $\mathbf{2}^{\mathbf{SS}}$

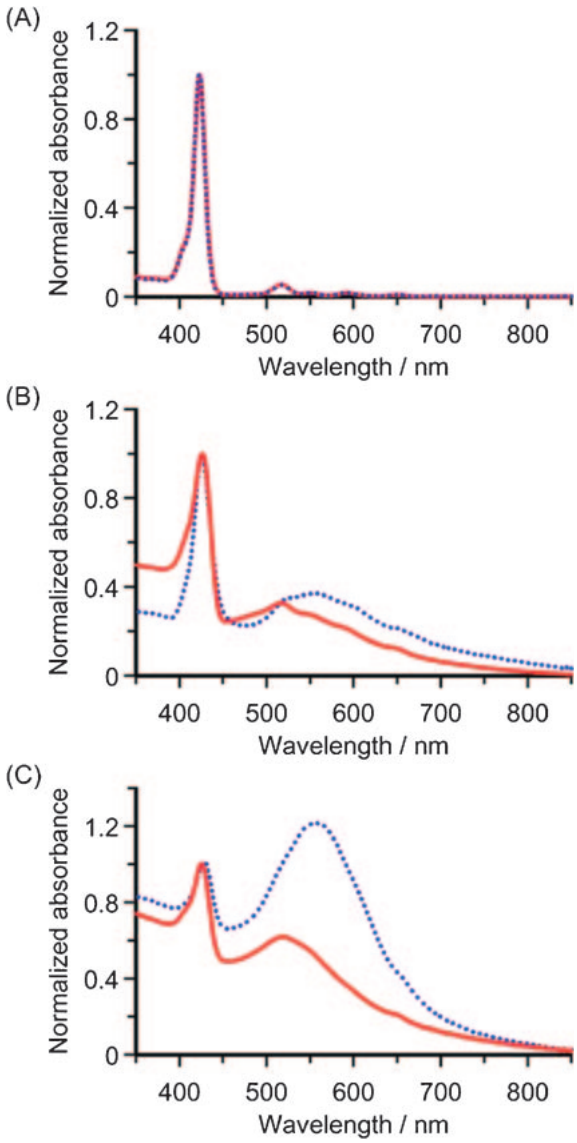

Figure 2. Absorption spectra of $\mathbf{2}^{\mathbf{SAc}}$ and $\mathbf{2}^{\mathbf{SS}}$ (A) as well as $\mathbf{GN@2}^{\mathbf{SAc}}$ and $\mathbf{GN@2}^{\mathbf{SS}}$ prepared at the initial S/Au ratio = 1 (B) and 0.1 (C) in DMF. $\mathbf{2}^{\mathbf{SAc}}$ and its derivatives are drawn in blue dotted lines and $\mathbf{2}^{\mathbf{SS}}$ and its derivatives in red.

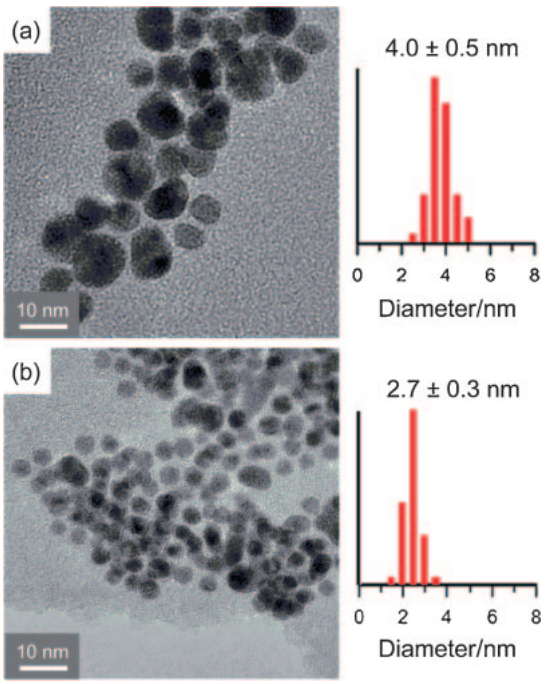

Figure 3. TEM images of **GN@2^{SAc}** (a) and **GN@2^{SS}** (b) with histograms of particle size on the right. Initial S-to-Au ratio = 1 for both cases.

should afford smaller gold nanoparticles than *S*-thioester passivants **1^{SAc}** and **2^{SAc}** under identical conditions. Although Kanehara and co-workers reported that the molar absorption coefficients of the Soret bands for **SC$_n$P** decrease by one order of magnitude upon coordination onto the gold nanoparticles,[17] **GN@2^{SS}** did not show such a large decrease in the intensity of the Soret band ($\varepsilon_{Soret} = 3.4 \times 10^5$ and $1.1 \times 10^5\,M^{-1}\,cm^{-1}$ for **2^{SS}** and **GN@2^{SS}** in DMF, respectively, where the latter value was obtained by subtracting the surface plasmon band derived from gold nanoparticles), indicating weaker interactions between **2^{SS}** and gold nanoparticles due to the longer arms of **2^{SS}** than **SC$_n$P**.

Next, we prepared gold nanoparticles under more severe conditions, that is, at $\xi = 0.1$ (Figure 2C). Under this condition, reduction of $HAuCl_4$ gave a clear red solution in both cases. A DMF solution of purified **GN@2^{SAc}** ($\xi = 0.1$) showed a much more intense surface plasmon band at ca. 562 nm than that of **GN@2^{SAc}** ($\xi = 1$), but the UV–vis spectrum of **GN@2^{SS}** ($\xi = 0.1$) did not differ greatly from that of **GN@2^{SS}** ($\xi = 1$). This result indicated that the particle size of **GN@2^{SAc}** increased with a decrease in the ratio of initially used S to Au (ξ), but that the particle size of **GN@2^{SS}** was nearly constant despite the changing ξ value.

Particle Size. To further evaluate the ability of **2^{SS}** to cap small gold nanoparticles, we estimated the particle size of **GN@2^{SAc}** and **GN@2^{SS}** prepared at five different ξ values by TEM measurements. Representative TEM images of **GN@2^{SAc}** and **GN@2^{SS}** are shown in Figure 3, together with corresponding histograms of particle size distribution. Analyzed particle sizes (diameter in nm) are plotted against ξ in Figure 4. The particle size of **GN@2^{SAc}** decreased from 6.2 ± 1.4 nm and reached approximately 2 nm as the ξ value changed from 0.1 to

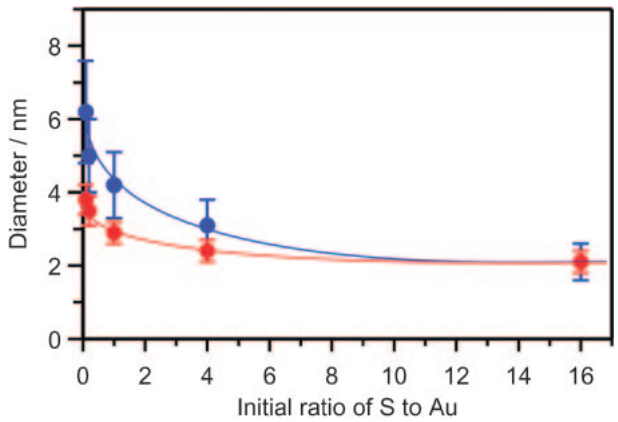

Figure 4. Mean diameter plots of gold nanoparticles **GN@2^{SAc}** (blue) and **GN@2^{SS}** (red) against the initial S-to-Au ratio.

16, which is very similar to that observed for **GN@1^{SAc}**.[23] On the other hand, the particle size of **GN@2^{SS}** was 3.8 ± 0.4 nm even at $\xi = 0.1$ and reached ca. 2 nm as the ξ value increased. This clearly demonstrates that the disulfide passivant **2^{SS}** efficiently capped the small growing gold nanoparticles.

Coverage Numbers. X-ray photoelectron spectra (XPS) of **GN@2^{SAc}** and **GN@2^{SS}** showed an S(2p) peak at the same binding energy of 163 eV, which is also the previously reported value for **GN@1^{SAc}**.[23] These results indicate that the ligands of both **2^{SA}** and **2^{SS}** attach to gold nanoparticles via four S–Au bonds; this consequently suggests, based on the molecular structure of the ligands, horizontal orientation of the porphyrin plane to the gold surface. In the XPS experiments, we also estimated the molar ratio of S to Au of **GN@2^{SS}** by dividing the peak areas of S(2p) and Au(4f) by the respective atomic sensitivity factors;[29] we found a molar ratio of 0.12 for **GN@2^{SS}** ($\xi = 1$). Since one 2.7-nm gold nanoparticle is composed of ca. 598 gold atoms, the S/Au ratio of 0.12 suggests that 18 porphyrin molecules cover the gold core of **GN@2^{SS}**, which agrees well with the model in which 18 porphyrin planes of ca. 1.25 nm^2 fully covered the particle surface. Horizontal full coverage with **2^{SS}** was also supported by elemental analysis. The values for elemental analysis of **GN@2^{SS}** (H, 0.80%; C, 10.92%; N, 1.48%) also support the model there are 18 porphyrin planes on the gold surface.

Aggregation of Gold Nanoparticles. Interestingly, the TEM images showed submicrometer-sized aggregates of gold nanoparticles when a suspension of purified **GN@2^{SS}** ($\xi = 1$) in MeOH was cast on a TEM grid to be dried (Figure 5), although samples prepared by evaporation of a drop of a DMF solution of **GN@2^{SS}** afforded discretely distributed gold nanoparticles as shown in Figure 3. The assembly of **GN@2^{SS}** seems to have a multi-layered structure. This behavior should be caused by the hydrophobic coating and uniform size of **GN@2^{SS}**.[30–36]

Conclusion

The constancy in particles size at S/Au ratio less than 4 was improved by the use of tetradentate disulfide passivant **2^{SS}** compared to the case of tetradentate *S*-thioester ligand **2^{SAc}**, which should be attributed to faster adsorption of disulfide

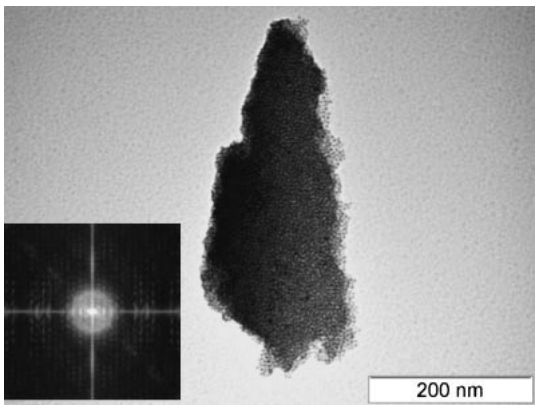

Figure 5. TEM images of submicrometer-sized assembly of **GN@2^{SS}** Inset: Fast Fourier transform of the image.

groups with gold than that of *S*-thioester groups. This effect is prominent because **2^{SS}** can yield ca. 3-nm gold nanoparticles even in the presence of a large number of Au^{III} ions. The result described here suggests that passivants having multivalent disulfide bonds should be promising candidates for constructing monolayer-protected gold nanoparticles of well-defined size.

This work was financially supported by Grants-in-Aid for Young Scientists (B) (Nos. 17750156 and 20750135) from the Ministry of Education, Culture, Sports, Science and Technology, Japan. J.O. thanks the JSPS Research Fellowships for Young Scientists.

Supporting Information

NMR spectra of **2^{SAc}** and **2^{SS}**, TEM images and XPS spectra of **GN@2^{SS}** and **GN@2^{SAc}**. This material is available free of charge on the web at http://www.csj.jp/journals/bcsj/.

References

1 P. K. Jain, X. Huang, I. H. El-Sayed, M. A. El-Sayed, *Acc. Chem. Res.* **2008**, *41*, 1578.

2 M. Hu, J. Chen, Z.-Y. Li, L. Au, G. V. Hartland, X. Li, M. Marquez, Y. Xia, *Chem. Soc. Rev.* **2006**, *35*, 1084.

3 M.-C. Daniel, D. Astruc, *Chem. Rev.* **2004**, *104*, 293.

4 J. Turkevich, P. C. Stevenson, J. Hillier, *Discuss. Faraday Soc.* **1951**, *11*, 55.

5 G. Frens, *Nature (London), Phys. Sci.* **1973**, *241*, 20.

6 M. Giersig, P. Mulvaney, *Langmuir* **1993**, *9*, 3408.

7 M. Brust, M. Walker, D. Bethell, D. J. Schiffrin, R. Whyman, *J. Chem. Soc., Chem. Commun.* **1994**, 801.

8 D. V. Leff, P. C. Ohara, J. R. Heath, W. M. Gelbart, *J. Phys. Chem.* **1995**, *99*, 7036.

9 M. J. Hostetler, J. E. Wingate, C.-J. Zhong, J. E. Harris, R. W. Vachet, M. R. Clark, J. D. Londono, S. J. Green, J. J. Stokes, G. D. Wignall, G. L. Glish, M. D. Porter, N. D. Evans, R. W. Murray, *Langmuir* **1998**, *14*, 17.

10 A. I. Frenkel, S. Nemzer, I. Pister, L. Soussan, T. Harris, Y. Sun, M. H. Rafailovich, *J. Chem. Phys.* **2005**, *123*, 184701.

11 A. C. Templeton, W. P. Wuelfing, R. W. Murray, *Acc. Chem. Res.* **2000**, *33*, 27.

12 T. Inomata, K. Konishi, *Chem. Commun.* **2003**, 1282.

13 K. Konishi, F. Xu, Y. Murakami, *Chem. Lett.* **2006**, *35*, 476.

14 S. Berner, S. Biela, G. Ledung, A. Gogoll, J.-E. Bäckvall, C. Puglia, S. Oscarsson, *J. Catal.* **2006**, *244*, 86.

15 P. D. Beer, D. P. Cormode, J. J. Davis, *Chem. Commun.* **2004**, 414.

16 P. D. Beer, S. R. Bayly, *Top. Curr. Chem.* **2005**, *255*, 125.

17 M. Kanehara, H. Takahashi, T. Teranishi, *Angew. Chem., Int. Ed.* **2008**, *47*, 307.

18 K. Wojczykowski, D. Meißner, P. Jutzi, I. Ennen, A. Hütten, M. Fricke, D. Volkmer, *Chem. Commun.* **2006**, 3693.

19 L. Srisombat, J.-S. Park, S. Zhang, T. R. Lee, *Langmuir* **2008**, *24*, 7750.

20 S. Zhang, G. Leem, L. Srisombat, T. R. Lee, *J. Am. Chem. Soc.* **2008**, *130*, 113.

21 L. Srisombat, S. Zhang, T. R. Lee, *Langmuir* **2010**, *26*, 41.

22 R. Balasubramanian, B. Kim, S. L. Tripp, X. Wang, M. Lieberman, A. Wei, *Langmuir* **2002**, *18*, 3676.

23 T. Peterle, A. Leifert, J. Timper, A. Sologubenko, U. Simon, M. Mayor, *Chem. Commun.* **2008**, 3438.

24 J. Ohyama, Y. Hitomi, Y. Higuchi, M. Shinagawa, H. Mukai, M. Kodera, K. Teramura, T. Shishido, T. Tanaka, *Chem. Commun.* **2008**, 6300.

25 J. P. Collman, X. M. Zhang, P. C. Herrmann, E. S. Uffelman, B. Boitrel, A. Straumanis, J. I. Brauman, *J. Am. Chem. Soc.* **1994**, *116*, 2681.

26 R. J. Abraham, G. E. Hawkes, M. F. Hudson, K. M. Smith, *J. Chem. Soc., Perkin Trans. 2* **1975**, 204.

27 M. I. Béthencourt, L. Srisombat, P. Chinwangso, T. R. Lee, *Langmuir* **2009**, *25*, 1265.

28 J. M. Tour, L. Jones, II, D. L. Pearson, J. J. S. Lamba, T. P. Burgin, G. M. Whitesides, D. L. Allara, A. N. Parikh, S. Atre, *J. Am. Chem. Soc.* **1995**, *117*, 9529.

29 J. E. Redman, J. K. M. Sanders, *Org. Lett.* **2000**, *2*, 4141.

30 C. D. Wagner, W. M. Riggs, L. E. Davis, J. M. Moulder, *Handbook of X-ray Photoelectron Spectroscopy*, ed. by G. E. Muilenberg, Perkin-Elmer Co., Eden Prairie, MN, USA, **1979**.

31 *Nanoparticle Assemblies and Superstructures*, ed. by N. A. Kotov, CRC Press, Boca Raton, FL, **2005**.

32 J. Vignolle, T. D. Tilley, *Chem. Commun.* **2009**, 7230.

33 H. Yao, H. Kojima, S. Sato, K. Kimura, *Langmuir* **2004**, *20*, 10317.

34 M. Kanehara, E. Kodzuka, T. Teranishi, *J. Am. Chem. Soc.* **2006**, *128*, 13084.

35 A. Wei, *Chem. Commun.* **2006**, 1581.

36 B. Kim, S. L. Tripp, A. Wei, *J. Am. Chem. Soc.* **2001**, *123*, 7955.